Am J Transl Res 2026;18(11):9888-9896
www.ajtr.org /ISSN:1943-8141/AJTR0175364

Original Article

Perfusion CT qualitative features combined with systemic immune-inflammation index for predicting malignancy risk in indeterminate pulmonary nodules

Kai Feng[1], Wenqin Li[1], Guifang Xia[1], Jianglong Li[1], Caimei Chen[1], Zhiyun Han[2], Yinliang Deng[1]

[1]Department of Medical Imaging, Yingtan 184 Hospital, China RongTong Medical Healthcare Group Co. Ltd., Yingtan 335000, Jiangxi, China; [2]Department of Radiology, The First Affiliated Hospital of Changsha Medical University, Changsha 410219, Hunan, China

Received July 14, 2026; Accepted September 29, 2026; Epub November 15, 2026; Published November 30, 2026

Abstract: Objective: To evaluate the clinical utility of qualitative perfusion CT features combined with the systemic immune-inflammation index (SII) for assessing the malignancy risk of indeterminate pulmonary nodules (IPN). Methods: A total of 228 patients with IPN were retrospectively enrolled as the model group and divided into benign and malignant groups according to pathological results. Besides, 120 patients were enrolled as the external verification group. Spiculation, lobulation, pleural retraction, and vascular convergence signs and inflammatory indices were compared between the benign and malignant groups. Multivariate logistic regression was used to identify independent risk factors, and a combined prediction model was constructed. ROC curve analysis was used to evaluate the predictive performance of the model. Results: The malignant group exhibited higher detection rates of spiculation, lobulation, pleural retraction, and vascular convergence signs than the benign group (all P<0.05). Additionally, NEU, PLT, and SII levels were higher, while lymphocytes were lower in the malignant group (all P<0.05). Multivariate logistic regression identified spiculation, lobulation, pleural retraction, vascular convergence, and SII as independent predictors of IPN malignancy (P<0.05). ROC analysis revealed that the AUCs for predicting IPN malignancy were 0.743 for spiculation, 0.693 for lobulation, 0.661 for pleural retraction, 0.674 for vascular convergence, and 0.854 for SII. The combined model integrating these factors achieved an AUC of 0.944. Conclusion: Qualitative perfusion CT features combined with SII can improve the identification of malignant risk in IPN and they have good predictive performance and clinical application value.

Keywords: Indeterminate pulmonary nodule, perfusion CT, systemic immune-inflammation index, risk factors, predictive value

Introduction

As low-dose computed tomography (CT) becomes increasingly used for lung cancer screening, the detection of pulmonary nodules continues to rise annually. Although the majority of these nodules are benign, a considerable proportion cannot be clearly classified as benign or malignant based on imaging features, density, or growth patterns, and are therefore categorized as indeterminate pulmonary nodules (IPN) [1, 2]. Traditional CT evaluation of lung nodules relies mainly on nodule size, margin characteristics, density, and growth during follow-up. However, for IPN with atypical morphological features or slow changes, these indicators have limited differential value and can easily lead to excessive follow-up, delayed diagnosis, or unnecessary invasive procedures [3, 4]. Therefore, exploring new imaging methods that can reflect the biological behavior of nodules is of great clinical significance. Perfusion CT is a functional imaging technique that can indirectly reflect tumor angiogenesis and microcirculation by analyzing tissue blood flow, blood volume, and enhancement patterns [5, 6]. Previous studies have shown that malignant lung nodules are often characterized by high or uneven perfusion because of the rich and abnormal structure of new blood vessels, providing a new imaging basis for differentiating benign from malignant

https://doi.org/10.62347/XRUK2276

Table 1. Comparison of general information between groups

General information		Malignant group (n=130)	Benign group (n=98)	t/χ^2	P
Age (years)		63.18±8.33	62.43±9.26	0.641	0.522
Gender	Male	76 (58.46)	50 (51.02)	1.251	0.263
	Female	54 (41.54)	48 (48.98)		
BMI (kg/m^2)		23.95±3.16	23.42±2.96	1.288	0.199
Smoking history		62 (47.69)	39 (39.80)	1.412	0.235
Hypertension		51 (39.23)	33 (33.67)	0.742	0.389
Diabetes		25 (19.23)	16 (16.33)	0.320	0.572
Number of nodules	Single	112 (86.15)	83 (84.69)	0.096	0.756
	Multiple	18 (13.85)	15 (15.31)		

Note: BMI: Body mass index.

Table 2. Comparison of perfusion CT qualitative features between groups (n, %)

Characteristic	Malignant group (n=130)	Benign group (n=98)	χ^2	P
Spiculation sign	95 (73.08)	24 (24.49)	52.866	<0.001
Lobulation sign	86 (66.15)	27 (27.55)	33.309	<0.001
Pleural retraction sign	67 (51.54)	19 (19.39)	24.587	<0.001
Vascular convergence sign	73 (56.15)	21 (21.43)	27.808	<0.001
Cavity sign	14 (10.77)	11 (11.22)	0.012	0.913

lung nodules [7, 8]. However, local imaging features alone still cannot fully reflect the overall biological behavior of tumors. Tumor-related systemic inflammation plays an important role in the occurrence, development, and metastasis of tumors. The systemic immune-inflammation index (SII) integrates neutrophils (NEU), platelets (PLT), and lymphocytes (LYM) and can stably reflect the inflammatory state and immune balance of the body [9, 10]. Numerous studies have demonstrated that SII has value in the diagnosis, staging, and prognostic evaluation of various malignancies [11, 12]; however, its use in predicting the malignancy risk of IPN has rarely been reported. In this study, we combined qualitative perfusion CT features with SII to evaluate the malignant risk of IPN and develop a more accurate and practical risk prediction model.

Patients and methods

Patients

We retrospectively enrolled 228 patients with IPN who underwent perfusion CT at Yingtan 184 Hospital from June 2022 to March 2025 as the model group. Inclusion criteria: chest CT showed single or multiple indeterminate pulmonary nodules with a maximum diameter of ≤30 mm; perfusion CT examination was completed and the image quality met the analysis requirements; a complete routine blood test was performed within 1 week before the examination; and clinical and imaging data were complete. Exclusion criteria: history of any malignant tumor; concurrent acute infection, hematological disease, or autoimmune disease; previous chemoradiotherapy, immunotherapy, or hormone therapy; and perfusion CT images with obvious artifacts that could not be evaluated.

According to the pathological diagnosis, patients in the model group were divided into a benign group (n=98) and a malignant group (n=130). The pathological diagnoses in the malignant group included 121 cases of invasive lung adenocarcinoma, 39 cases of invasive squamous cell carcinoma, 16 cases of minimally invasive adenocarcinoma, 8 cases of adenocarcinoma in situ, and 8 cases of other malignant tumors. To verify the stability and generalizability of the model, 120 patients with IPN who met the research criteria from September 2024 to December 2025 were additionally enrolled as the external verification group. The inclusion and exclusion criteria, perfusion CT protocol, and laboratory testing methods for the external verification group were identical to those for the model group.

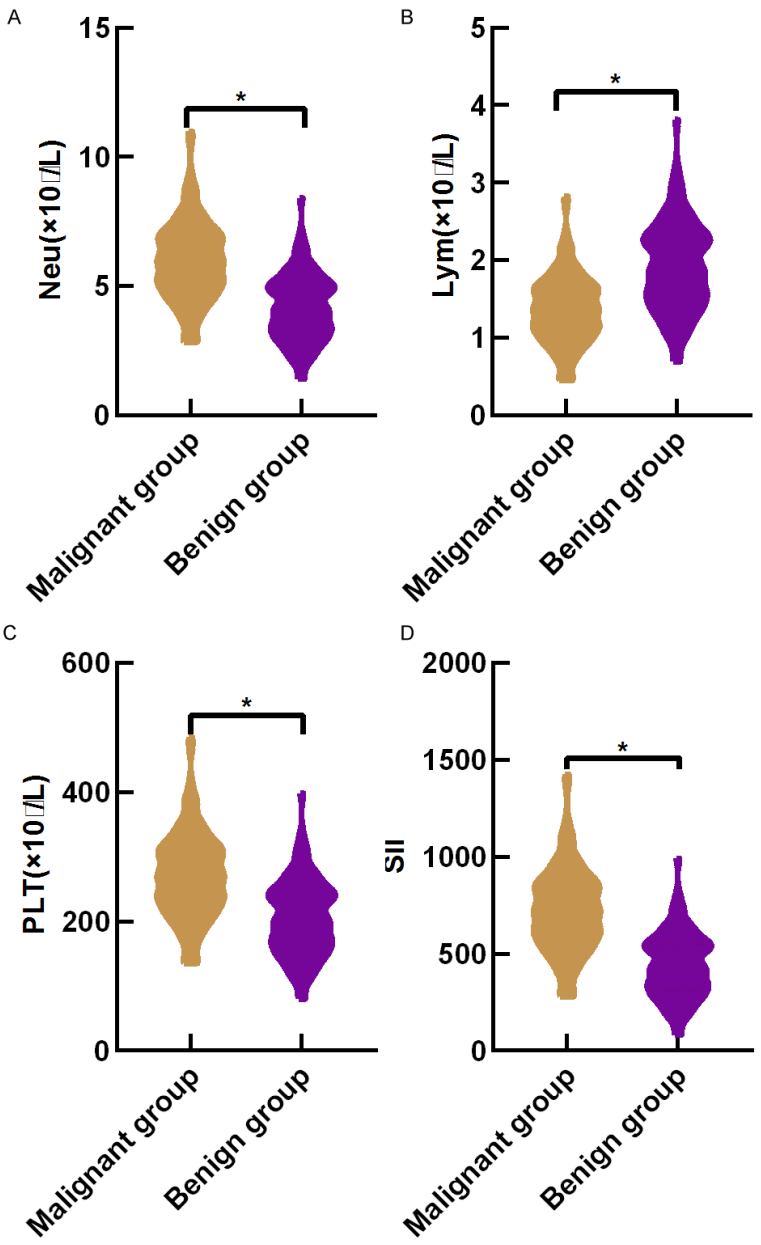


Figure 1. Comparison of inflammatory indices between the two groups. A: Comparison of NEU levels between two groups; B: Comparison of LYM levels between two groups; C: Comparison of PLT levels between two groups; D: Comparison of SII levels two groups. Note: *P<0.05 for between-group comparisons. NEU: neutrophils; LYM: lymphocytes; PLT: platelets; SII: systemic immune inflammation index.

Table 3. Variable assignment for multivariate analysis

Factor	Variable	Assignment
Spiculation sign	X1	1 = yes; 0 = no
Lobulation sign	X2	1 = yes; 0 = no
Pleural retraction sign	X3	1 = yes; 0 = no
Vascular convergence sign	X4	1 = yes; 0 = no
SII	X5	Continuous variable

Note: SII: systemic immune inflammation index.

Study methods

Perfusion CT examination: A Brilliance 64-slice spiral CT scanner (Philips, the Netherlands) was used. Nonionic contrast medium (approximately 40-50 mL) was injected into the antecubital vein at a flow rate of 4-5 mL/s, followed by dynamic contrast-enhanced scanning. Two radiologists with more than 5 years of experience independently reviewed the images without knowledge of the pathological results; if discrepancies arose, a third senior physician made the final decision. The qualitative features assessed included spiculation, lobulation, pleural retraction, vascular convergence, and cavity sign. Each feature was recorded as present or absent.

Inflammatory markers: Peripheral venous blood samples were obtained from all patients within 24 hours of admission. Routine blood parameters, including NEU, LYM, and PLT, were measured using an automated hematology analyzer. SII=PLT×NEU/LYM.

Statistical analysis

SPSS 22.0 was used for all statistical analyses, and GraphPad Prism 8 was used for figure illustration. Categorical data were expressed as rates and compared using the chi-square test. Continuous variables were compared between groups using the t-test. Multivariate analysis was performed using logistic regression. The predictive value of perfusion CT qualitative features and SII for IPN malignancy was evaluated using Receiver Operating Characteristic (ROC) curve analysis. A *P*-value of less than 0.05 was considered statistically significant.

Table 4. Multivariate analysis of risk factors for IPN malignancy

Factor	β	SE	Wald	Sig.	Exp(B)	95% CI
Constant	-4.836	0.721	44.982	<0.001	0.008	-
Spiculation sign	0.921	0.286	10.367	<0.001	2.512	1.432-4.407
Lobulation sign	0.768	0.274	7.850	0.005	2.155	1.257-3.696
Pleural retraction sign	0.693	0.292	5.634	0.018	2.001	1.128-3.546
Vascular convergence sign	0.641	0.281	5.203	0.023	1.899	1.097-3.286
SII	0.251	0.051	24.220	<0.001	1.285	1.163-1.420

Note: SII: systemic immune inflammation index.

Table 5. Predictive value of each index for IPN malignancy

Predictive indexes	AUC	95% CI	Youden index	Sensitivity (%)	Specificity (%)	Cut-off value
Spiculation sign	0.743	0.677-0.809	0.486	75.51	73.08	-
Lobulation sign	0.693	0.623-0.763	0.386	72.45	66.15	-
Pleural retraction sign	0.661	0.590-0.732	0.321	80.61	51.54	-
Vascular convergence sign	0.674	0.603-0.744	0.347	78.57	56.15	-
SII	0.854	0.805-0.902	0.588	85.71	73.08	596.00
Combined prediction	0.944	0.917-0.971	0.754	96.94	78.46	0.695

Note: SII: systemic immune inflammation index.

Results

Comparison of general information between groups

There was no significant difference in general information between the two groups (all P>0.05). See **Table 1**.

Comparison of perfusion CT qualitative features between groups

The malignant group showed higher detection rates of spiculation, lobulation, pleural retraction, and vascular convergence signs compared with the benign group (all P<0.05). See **Table 2**.

Comparison of inflammatory indices between groups

The levels of NEU, PLT, and SII were higher in the malignant group than those in the benign group, while the LYM level was lower (all P<0.05). See **Figure 1**.

Multivariate analysis of risk factors for IPN malignancy

The independent variables were coded as shown in **Table 3**. Multivariate analysis identified spiculation, lobulation, pleural retraction, vascular convergence, and SII as independent predictors of IPN malignancy (all P<0.05). See **Table 4**.

Predictive value of perfusion CT qualitative features combined with SII in predicting IPN malignancy

Spiculation, lobulation, pleural retraction, vascular convergence, and SII were entered into the logistic regression model, and the predicted probability of malignancy was used as the combined predictive index. ROC curve analysis showed that the predictive performance for IPN malignancy varied among the indicators. The Area Under the Curve (AUC) for spiculation was 0.743 (95% CI: 0.677-0.809), with a sensitivity of 75.51% and a specificity of 73.08% (Youden index = 0.486). The AUC for lobulation was 0.693 (95% CI: 0.623-0.763), with a sensitivity of 72.45% and a specificity of 66.15% (Youden index = 0.386). The AUC for pleural retraction was 0.661 (95% CI: 0.590-0.732), with a sensitivity of 80.61% and a specificity of 51.54% (Youden index = 0.321). The AUC for vascular convergence was 0.674 (95% CI: 0.603-0.744), with a sensitivity of 78.57% and a specificity of 56.15% (Youden index = 0.347). SII alone achieved an AUC of 0.854 (95% CI: 0.805-0.902), with a sensitivity of 85.71% and a specificity of 73.08% at the optimal cutoff of 596.00 (Youden index = 0.588). The combined model integrating imaging features and SII achieved the highest predictive performance, with an AUC of 0.944 (95% CI: 0.917-0.971), a sensitivity of 96.94%, a specificity of 78.46%,

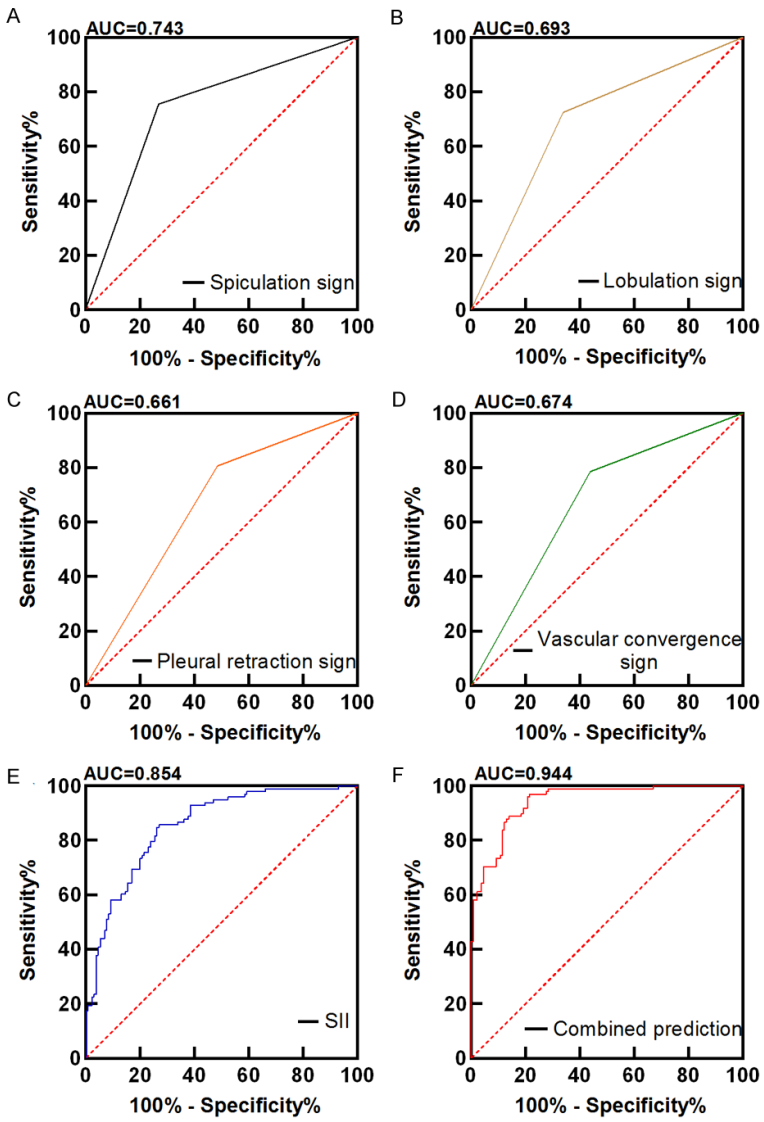


Figure 2. Predictive value of each index for IPN malignancy. A: spiculation sign; B: lobulation sign; C: pleural retraction sign; D: vascular convergence sign; E: SII; F: combined prediction. Note: SII: systemic immune inflammation index.

and a Youden index of 0.754. See **Table 5**; **Figure 2**.

Comparison of indicators between the external verification group and model group

No significant differences were found between the model group and the external verification group (all P>0.05), indicating good consistency between the two groups and confirming the stability and reliability of the model. See **Table 6**.

ROC curve analysis of external verification group

In the external verification group, the combined model achieved an AUC of 0.942, indicating that it maintained a the ability to identify malignant risk in an independent cohort, with satisfactory stability and generalizability. See **Table 7**; **Figure 3**.

Discussion

IPN is common in clinical practice, and differentiating benign from malignant IPN remains a major challenge in imaging and clinical decision-making. Over-reliance on invasive examinations may increase patient risk, whereas follow-up observation may delay the diagnosis and treatment of malignant lesions [13, 14]. Therefore, improving the accuracy of benign-malignant differentiation of IPN by non-invasive means has become a focus of current research. Perfusion CT has demonstrated unique advantages in reflecting tumor angiogenesis and hemodynamics, while SII reflects the systemic inflammatory and immune status associated with tumor occurrence and development [15, 16]. In this study, we combined qualitative perfusion CT features with SII to explore their clinical value in the risk assessment of benign and malignant IPN.

Analysis of perfusion CT qualitative features in this study revealed that spiculation, lobulation, pleural retraction, and vascular convergence signs were more frequently observed in the malignant group than in the benign group. These differences can be explained as follows. Spiculation usually reflects tumor infiltration into the surrounding interstitium, leading to

Table 6. Comparison of indicators between the external verification group and the model group

General information		Model group (n=228)	External verification group (n=120)	t/χ^2	P
Age (years)		62.86±9.65	62.51±7.77	0.343	0.732
Gender	Male	126	72	0.719	0.396
	Female	102	48		
BMI (kg/m^2)		23.64±3.42	23.15±3.22	1.296	0.196
Spiculation sign		119	70	1.195	0.274
Lobulation sign		113	66	0.931	0.335
Pleural retraction sign		86	51	0.753	0.386
Vascular convergence sign		94	58	1.614	0.204
Cavity sign		25	8	1.692	0.193
SII		829.18±442.84	868.33±423.15	0.796	0.427

Note: BMI: Body mass index; SII: systemic immune inflammation index.

Table 7. ROC curve analysis of the external verification group

Predictive indexes	AUC	95% CI	Youden index	Sensitivity (%)	Specificity (%)	Cut-off value
Spiculation sign	0.696	0.599-0.792	0.391	67.14	72.00	-
Lobulation sign	0.721	0.628-0.814	0.443	64.29	80.00	-
Pleural retraction sign	0.674	0.578-0.771	0.349	52.86	82.00	-
Vascular convergence sign	0.704	0.609-0.799	0.409	62.86	78.00	-
SII	0.848	0.776-0.92	0.614	91.43	70.00	604.2
Combined prediction	0.942	0.905-0.98	0.760	80.00	96.00	0.729

Note: SII: systemic immune inflammation index.

fibrous tissue reaction and interstitial traction. Lobulation suggests uneven tumor growth, which is closely related to regional differences in cell proliferation. Pleural retraction reflects fibrous connections or invasion between the tumor and the pleura. Vascular convergence indicates that tumor-induced neovascularization gathers toward the lesion. These signs reflect the pathological basis of aggressive growth and angiogenesis of malignant tumors from different perspectives and are therefore more common in malignant nodules [17, 18]. Regarding inflammatory markers, the malignant group exhibited elevated NEU, PLT, and SII levels and a lower LYM level than the benign group, which is closely related to the tumor-related inflammatory reaction and the immunosuppressive state of the body. As an important effector cell of the inflammatory response, NEU can be activated and recruited by various cytokines secreted by tumor cells in the tumor microenvironment. It promotes the proliferation, invasion, and metastasis of tumor cells by releasing reactive oxygen species and proteases and by promoting angiogenesis, thereby elevating the NEU level in patients with malignant nodules [19, 20]. PLT also plays a crucial role in tumor progression. They not only facilitate tumor angiogenesis through the release of various factors but also shield circulating tumor cells from immune clearance, thereby enhancing metastasis [21, 22]. This mechanism partly explains the elevated PLT levels observed in the malignant group. As the core component of antitumor immunity, LYM participates in the cellular immune response and directly kills tumor cells. During tumor progression, tumors can reduce the number and activity of lymphocytes by inducing immune tolerance and other mechanisms, which manifests as a decreased peripheral blood LYM levels [23, 24]. In addition, a long-term chronic inflammatory state may consume lymphocyte resources and further weaken the body's immune surveillance function. As a comprehensive index, SII more comprehensively reflects the imbalance between enhanced inflammatory response and suppressed immune function [25, 26]. Therefore, the increased SII level in the malignant group has a clear biological basis, further supporting its value in differentiating benign from malignant IPN.

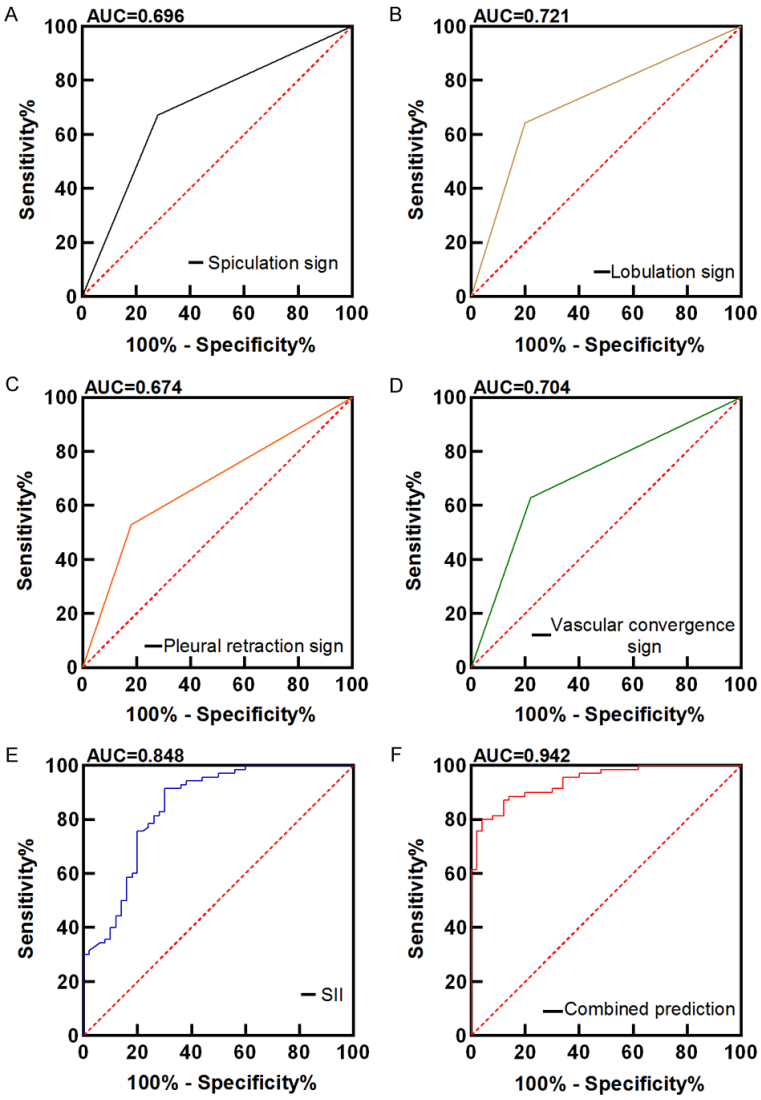


Figure 3. ROC curve analysis of the external verification group. A: Spiculation sign; B: Lobulation sign; C: Pleural retraction sign; D: Vascular convergence sign; E: SII; F: Combined prediction. Note: SII: systemic immune inflammation index.

Multivariate analysis indicated that spiculation, lobulation, pleural retraction, vascular convergence, and SII were independent predictors of IPN malignancy. These imaging signs reflect the invasive growth, intratumoral heterogeneity, and angiogenesis of malignant tumors, which are important biological characteristics of malignant nodules [27, 28]. SII is a comprehensive indicator of systemic inflammation and immune status. Its elevation indicates an enhanced pro-inflammatory response and weakened antitumor immune function, which explains why it serves as an important independent predictor of IPN malignant risk.

ROC curve analysis in this study demonstrated that the AUCs for predicting IPN malignancy were 0.743 for spiculation, 0.693 for lobulation, 0.661 for pleural retraction, 0.674 for vascular convergence, and 0.854 for SII. The combined model achieved an AUC of 0.944, which was significantly better than any single indicator. This indicates that integrating multidimensional information can significantly improve the accuracy of identifying benign and malignant IPN. Imaging features directly reflect the morphology and local biological behavior of the tumor, while SII reflects the systemic inflammatory and immune status; the two complement each other and thus improve the overall predictive performance.

In summary, the qualitative perfusion CT features (spiculation, lobulation, pleural retraction, and vascular convergence) and SII are important factors influencing the malignant risk of IPN, among which SII has high individual predictive value. The combination of the two can significantly improve diagnostic efficiency, provide an important basis for individualized clinical decision-making, and has good prospects for clinical application.

Disclosure of conflict of interest

None.

Address correspondence to: Yinliang Deng, Department of Medical Imaging, Yingtan 184 Hospital, China RongTong Medical Healthcare Group Co. Ltd., Yingtan 335000, Jiangxi, China. E-mail: hlb184@163.com

References

[1] Paez R, Kammer MN, Tanner NT, Shojaee S, Heideman BE, Peikert T, Balbach ML, Iams WT,

Ning B, Lenburg ME, Mallow C, Yarmus L, Fong KM, Deppen S, Grogan EL and Maldonado F. Update on biomarkers for the stratification of indeterminate pulmonary nodules. Chest 2023; 164: 1028-1041.
[2] van den Broek JJ, van Gestel T, Kol SQ, van Geel AM, Geenen RWF and Schreurs WH. Dealing with indeterminate pulmonary nodules in colorectal cancer patients; a systematic review. Eur J Surg Oncol 2021; 47: 2749-2756.
[3] Paez R, Kammer MN and Massion P. Risk stratification of indeterminate pulmonary nodules. Curr Opin Pulm Med 2021; 27: 240-248.
[4] McGann KC, Khalil TA, Kammer MN, Ostrin EJ, Pass HI, Tsay JJ, Segal LN, Potter M, Deppen SA, Maldonado F and Grogan EL. Biomarkers for the diagnosis of indeterminate pulmonary nodules: are we there yet? J Thorac Dis 2025; 17: 6265-6282.
[5] Guo X, Jia X, Zhang D, Feng H, Dou Y and Shi G. Indeterminate pulmonary subsolid nodules in patients with no history of cancer: growing prediction, CT pattern, and pathological diagnosis. Diagn Interv Radiol 2022; 28: 230-238.
[6] Prosper AE, Kammer MN, Maldonado F, Aberle DR and Hsu W. Expanding role of advanced image analysis in CT-detected indeterminate pulmonary nodules and early lung cancer characterization. Radiology 2023; 309: e222904.
[7] Kim RY, Oke JL, Pickup LC, Munden RF, Dotson TL, Bellinger CR, Cohen A, Simoff MJ, Massion PP, Filippini C, Gleeson FV and Vachani A. Artificial intelligence tool for assessment of indeterminate pulmonary nodules detected with CT. Radiology 2022; 304: 683-691.
[8] Andersson E, Dai Ydrefelt Y, Johannesson M, Lundbäck M, Mannila M, Persson M, Swahn E and Bolejko A. Surveillance of indeterminate pulmonary nodules detected with CT in a Swedish population-based study (SCAPIS): psychosocial consequences and impact on health-related quality of life-a multicentre prospective cross-sectional study. BMJ Open 2021; 11: e048721.
[9] Zhou Y, Dai M and Zhang Z. Prognostic significance of the systemic immune-inflammation index (SII) in patients with small cell lung cancer: a meta-analysis. Front Oncol 2022; 12: 814727.
[10] Xu Y, Zhang L, Chen Z, Sun X, Zhao M, Wu Q and Hao J. The diagnostic value of systemic immune-inflammatory index (SII) and lymphocyte-albumin-neutrophil ratio (LANR) in chronic obstructive pulmonary disease with lung cancer. J Inflamm Res 2024; 17: 5555-5565.
[11] Yao B, Xia G, Zhao L, Ma K and Chen Z. SII and lung cancer in middle-aged and elderly population: the nonlinear connection and the mediating role of ABSI. World J Surg Oncol 2025; 23: 345.
[12] Miao Y, Li C, Zhang Y, Li Z, Li Y, Sun Y, Zheng X, Ai J, Liu L, You R, Tu C, Zhang T and Chen X. Perioperative changing patterns of systemic immune-inflammatory index (SII) and outcomes in stage I-III non-small cell lung cancer: a retrospective cohort study. J Thorac Dis 2025; 17: 8410-8420.
[13] Hassan MS, Ariyaratne S, Azzopardi C, Iyengar KP, Davies AM and Botchu R. The clinical significance of indeterminate pulmonary nodules in patients with primary bone sarcoma: a systematic review. Br J Radiol 2024; 97: 747-756.
[14] Franco J, Galán G, Bondía E, Pastor I, Calderón A, Insa A, Mollá MÁ, Martín-Martorell P, Carbonell JA and Signes-Costa J. Indeterminate pulmonary nodules and prior malignancy: survival and recurrence after surgery in newly diagnosed stage I non-small cell lung cancer. J Thorac Dis 2024; 16: 2757-2766.
[15] Zhang C, Zhou H, Li M, Yang X, Liu J, Dai Z, Ma H and Wang P. The diagnostic value of CT-based radiomics nomogram for solitary indeterminate smoothly marginated solid pulmonary nodules. Front Oncol 2024; 14: 1427404.
[16] Guo H, Li W, Wu W and Duan G. SII-CRP/Alb score was used to determine the prognosis of postoperative patients with non-small cell lung cancer. Asian J Surg 2023; 46: 5149-5150.
[17] Hanaoka T, Matoba H, Nakayama J, Ono S, Ikegawa K and Okada M. A spatio-temporal image analysis for growth of indeterminate pulmonary nodules detected by CT scan. Radiol Phys Technol 2024; 17: 71-82.
[18] Zhao M, Xue G, He B, Deng J, Wang T, Zhong Y, Li S, Wang Y, He Y, Chen T, Zhang J, Yan Z, Hu X, Guo L, Qu W, Song Y, Yang M, Zhao G, Yu B, Ma M, Liu L, Sun X, Zhao D, Xie D, Chen C and She Y. A multiomics dataset of paired CT image and plasma cell-free DNA end motif for patients with pulmonary nodules. Sci Data 2025; 12: 545.
[19] Salcher S, Sturm G, Horvath L, Untergasser G, Kuempers C, Fotakis G, Panizzolo E, Martowicz A, Trebo M, Pall G, Gamerith G, Sykora M, Augustin F, Schmitz K, Finotello F, Rieder D, Perner S, Sopper S, Wolf D, Pircher A and Trajanoski Z. High-resolution single-cell atlas reveals diversity and plasticity of tissue-resident neutrophils in non-small cell lung cancer. Cancer Cell 2022; 40: 1503-1520.e8.
[20] Tang Z, Hu J, Li XC, Wang W, Zhang HY, Guo YY, Shuai X, Chu Q, Xie C, Lin D and Zhong B. A subset of neutrophils activates anti-tumor immunity and inhibits non-small-cell lung cancer progression. Dev Cell 2025; 60: 379-395, e8.

[21] Walke V, Das S, Mittal A and Agrawal A. Tumor educated platelets as a biomarker for diagnosis of lung cancer: a systematic review. Asian Pac J Cancer Prev 2024; 25: 1911-1920.
[22] Li B, Zhu T, Wu X, Chen S, Lu C, Zhu J and Li Q. The crosstalk between lung cancer cells and platelets promotes tumor angiogenesis in vivo and in vitro. J Cancer Res Clin Oncol 2023; 149: 3495-3511.
[23] Xu Y, Li J, Ji X, Chen Q, Liu Z and Ji S. Lymphocyte-to-C-reactive protein ratio predicts prognosis in unresectable locally advanced non-small cell lung cancer patients. Ann Med 2025; 57: 2487629.
[24] Quan Z, Han Z, Yang Y, Wang J, Wang H, Yang L, A R, Hu X, Wang J, Li X, Li X, Yu H, Chen W, Wang K and Sun X. Noninvasive monitoring of immunotherapy in lung cancer by lymphocyte activation gene 3 PET imaging of tumor-infiltrating lymphocytes. J Nucl Med 2024; 65: 25-32.
[25] Cai M, Sun J, Wu J, Liu Y and Huang Y. Prognostic analysis and association of the systemic immune-inflammatory index with immune checkpoint inhibitor pneumonitis in patients with non-small cell lung cancer. Front Oncol 2025; 15: 1596223.
[26] Fu F, Deng C, Wen Z, Gao Z, Zhao Y, Han H, Zheng S, Wang S, Li Y, Hu H, Zhang Y and Chen H. Systemic immune-inflammation index is a stage-dependent prognostic factor in patients with operable non-small cell lung cancer. Transl Lung Cancer Res 2021; 10: 3144-3154.
[27] Podder S, Chaudry S, Singh H, Jondall EM, Kurman JS and Benn BS. Efficacy and safety of cone-beam CT augmented electromagnetic navigation guided bronchoscopic biopsies of indeterminate pulmonary nodules. Tomography 2022; 8: 2049-2058.
[28] Rundo L, Ledda RE, di Noia C, Sala E, Mauri G, Milanese G, Sverzellati N, Apolone G, Gilardi MC, Messa MC, Castiglioni I and Pastorino U. A low-dose CT-based radiomic model to improve characterization and screening recall intervals of indeterminate prevalent pulmonary nodules. Diagnostics (Basel) 2021; 11: 1610.